Thermodynamic Cycles as Probes of Structure in Unfolded Proteins[†,‡]

William A. McGee,[§] Frederico I. Rosell,[||] John R. Liggins,[§] Sofia Rodriguez-Ghidarpour,[§] Yaoguang Luo,[||] Jie Chen,[||] Gary D. Brayer,[||] A. Grant Mauk,[||] and Barry T. Nall*[,§]

Department of Biochemistry, University of Texas Health Science Center, San Antonio, Texas 78284-7760, and Department of Biochemistry and Molecular Biology, University of British Columbia, Vancouver, British Columbia, V6T 1Z3, Canada

Received June 1, 1995; Revised Manuscript Received September 21, 1995[⊗]

ABSTRACT: The relationship between structure and stability has been investigated for the folded forms and the unfolded forms of iso-2 cytochrome *c* and a variant protein with a stability-enhancing mutation, N52I iso-2. Differential scanning calorimetry has been used to measure the reversible unfolding transitions for the proteins in both heme oxidation states. Reduction potentials have been measured as a function of temperature for the folded forms of the proteins. The combination of measurements of thermal stability and reduction potential gives three sides of a thermodynamic cycle and allows prediction of the reduction potential of the thermally unfolded state. The free energies of electron binding for the thermally unfolded proteins differ from those expected for a fully unfolded protein, suggesting that residual structure modulates the reduction potential. At temperatures near 50 °C the N52I mutation has a small but significant effect on oxidation state-sensitive structure in the thermally unfolded protein. Inspection of the high-resolution X-ray crystallographic structures of iso-2 and N52I iso-2 shows that the effects of the N52I mutation and oxidation state on native protein stability are correlated with changes in the mobility of specific polypeptide chain segments and with altered hydrogen bonding involving a conserved water molecule. However, there is no clear explanation of oxidation state or mutation-induced differences in stability of the proteins in terms of observed changes in structure and mobility of the folded forms of the proteins alone.

The two parts to understanding the structural basis of protein stability are (1) the structure of the folded protein and (2) the competing structure, or lack thereof, within the unfolded protein. Characterization of any pre-existing structure in the unfolded state is necessary for a full understanding of protein stability. Residual structure retained in an unfolded protein may also be important in facilitating folding rates. The known rates of folding are much too fast for folding to occur by an exhaustive search of all potential conformations (Creighton, 1994; Levinthal, 1968; Zwanzig et al., 1992). So how does a protein find the native conformation so quickly? One proposal is that a hydrophobically driven nonspecific collapse of the polypeptide drastically reduces the number of conformations explored by a folding polypeptide chain (Dill, 1985). Another possibility is that an unfolded polypeptide differs from the "random coil" of the polymer chemist by retaining folding information as residual structure, so that aspects of the functional ordered state are present within the unfolded protein (Furie et al., 1975; Sachs et al., 1972). Conformational preferences retained within a structured unfolded polypeptide might provide a memory of the functional, three-dimensional structure of the native protein and serve as guideposts that channel the polypeptide along a productive path to the native state.

Here we present an approach to characterizing the unfolded state of cytochrome *c* which emphasizes the functional aspects of the native protein. A thermodynamic cycle is used to measure a property of unfolded cytochrome *c* inaccessible to direct measurement: the reduction potential of thermally unfolded cytochrome *c*. Standard thermodynamic relationships allow the extension of the results to conditions that strongly favor protein refolding. When combined with site-directed mutagenesis (Zoller & Smith, 1983), the mapping of functionally relevant interactions in unfolded proteins becomes feasible. A very similar approach based on the linkage between protein stability, disulfide bonds, and the oxidation reduction potentials of free sulfhydryls has been used to assess effects of mutations on folded and unfolded forms of thioredoxin (Lin & Kim, 1989, 1991; Wynn & Richards, 1993) and T4 lysozyme (Lu et al., 1992).

The relationship between electron binding and the thermodynamic stability of cytochrome *c* is well known (Pfeil, 1981). Recently, this relationship was employed to obtain indirect measures of the stability of reduced iso-1 cytochrome *c* (Komar-Panicucci et al., 1994). Our approach differs by measuring the stability of the reduced protein directly. Combined with scanning calorimetry measurements of the oxidized protein and measurements of the temperature dependence of the reduction potential of the native protein, three sides of a thermodynamic cycle are obtained which allow calculation of the free energy of electron binding for the unfolded protein. Surprisingly, electron binding is

[†] Supported by grants from the National Institute of General Medical Sciences, GM32980 (B.T.N.), GM33804 (A.G.M.), the National Center for Research Resources, RR05043 (B.T.N.), and the Robert A. Welch Foundation, AQ838 (B.T.N.). X-ray diffraction studies were supported by an operating grant from the Medical Research Council (G.D.B.) and utilized equipment purchased as part of the National Centers of Excellence Program in Protein Engineering (Canada).

[‡] The coordinates for reduced N52I iso-2 and iso-2 have been deposited in the Protein Data Bank (Bernstein et al., 1977) under the identification codes 1YTC and 1YEA, respectively. The structure of reduced iso-2 was reported previously (Murphy et al., 1992).

* Address correspondence to this author at the Department of Biochemistry, University of Texas Health Science Center, 7703 Floyd Curl Drive, San Antonio, TX 78284-7760. Telephone: (210) 567-6621. Fax: (210) 567-6595. E-mail: nall@bioc01.uthscsa.edu.

[§] University of Texas Health Science Center.

[||] University of British Columbia.

[⊗] Abstract published in *Advance ACS Abstracts,* January 15, 1996.

0006-2960/96/0435-1995$12.00/0

significantly better than would be expected for a structureless unfolded state with histidine heme ligands. Similar measurements are made with a global suppressor mutant protein, N52I iso-2 cytochrome *c*. These results show that the N52I mutation weakens electron binding to both folded and unfolded forms of iso-2 cytochrome *c*.

The second part of the structure stability relationship is the folded protein. Is a structural basis discernible for the large difference in stability between the oxidized and reduced forms of cytochrome *c*? Is there a structural explanation for how the N52I global suppressor mutation enhances protein stability, while it diminishes electron binding affinity? X-ray crystallographic studies on iso-1, N52I iso-1, and other iso-1 variant proteins in both oxidation states (Berghuis et al., 1994) have provided a wealth of structural detail that can be used to distinguish between possible models. The structural basis for understanding electron binding affinity and protein stability has been extended further by X-ray studies of reduced iso-2 (Murphy et al., 1992; Murphy, 1993) and in our studies herein of the N52I iso-2 variant protein.

MATERIALS AND METHODS

Site-Directed Mutagenesis. Construction of the N52I iso-2 mutant was carried out as described (Guillemette et al., 1994; Inglis et al., 1991) for site-directed mutagenesis and expression of the yeast iso-1 cytochrome *c* gene. A difference was that our experiments involved mutagenesis of a 0.6 kb *Sau*3A fragment of DNA containing the structural gene (CYC7) for the iso-2 isozyme of yeast cytochrome *c* (Montgomery et al., 1980). The cloning vector for the yeast iso-2 cytochrome *c* gene (CYC7) was constructed by inserting the *Sau*3A fragment carrying the CYC7 gene into the *Bam*HI site of the yeast *E. coli* phagemid, pEMBLYe30. The pEMBLYe30-CYC7 phagemid has the advantage that the same cloning vector can be used to prepare double-stranded plasmid DNA in *Escherichia coli*, to express the iso-2 cytochrome *c* protein in the yeast, and to prepare single-strand template DNA for site-directed mutagenesis and DNA sequencing. Mutant genes were identified by dideoxy-DNA sequencing.

Protein Isolation and Characterization. Yeast (*Saccharomyces cerevisiae*) were grown, and iso-2-cytochrome *c* was isolated as described previously (Nall & Landers, 1981; Wood et al., 1988; Zuniga & Nall, 1983). After lyophilization the purified proteins were stored at −70 °C until needed for sample preparation. The primary structures of the purified proteins were verified by electrospray ion mass spectrometry.

X-ray Diffraction Structural Studies. Crystals of the N52I iso-2 cytochrome *c* mutant in the reduced state were grown as previously described for the wild type protein (Murphy et al., 1992) from a solution containing 20 mg/mL protein, 0.1 M sodium phosphate buffer (pH 7.0), 0.3 M NaCl, 40 mM dithiothreitol, and 90% saturated $(NH_4)_2SO_4$. The crystals obtained were found to be isomorphous with their wild type protein counterparts, and the observed unit cell parameters are summarized in Table 1. Diffraction data were collected to 1.8 Å resolution from a single crystal of N52I iso-2 cytochrome *c* using a Rigaku R-Axis II imaging plate area detector mounted on a RU-300 rotating anode generator operating at 100 mA and 60 kV. For each data collection frame, the crystal was oscillated through a phi angle of 1.0° and exposed to the X-ray beam for 14 min. X-ray intensity data were processed to structure factors (Higashi, 1990; Sato et al., 1992) and put on an absolute scale using the Wilson plot method (Wilson, 1942).

Table 1: Data Collection and Refinement Parameters

I. Data Collection	
space group	$P4_32_12$
cell dimensions (Å)	
$a = b$	36.66
c	138.92
resolution range (Å)	∞−1.8
total no. of reflections collected	59573
no. of unique reflections	9141
data completeness	
overall	95.5%
outer shell (2.0−1.8 Å)	93.4%
merging R factor (%)[a]	6.0
II. Refinement	
no. of reflections used	8985
resolution range (Å)	8.0−1.8
no. of protein atoms	917
no. of solvent molecules	117
average thermal factors (Å^2)	
protein atoms	21.6
solvent atoms	40.7
final refinement R factor (%)[b]	16.2

[a] $R_{merge} = (\sum_{hkl}\sum_{i=1}^{n}|I_{i_{hkl}} - \bar{I}_{hkl}|)/(\sum_{hkl}\sum_{i=1}^{n}I_{hkl})$. [b] $R_{cryst} = (\sum_{hkl}|F_o - F_c|)/(\sum_{hkl}|F_o|)$.

An initial refinement model of N52I iso-2 cytochrome *c* was constructed using the coordinates of the refined wild type protein (Murphy et al., 1992) with residue 52 truncated to an alanine. In the first phase of refinement the program X-PLOR (Brunger, 1992) was used to refine individual atomic positional and thermal factor parameters. Following this, $F_o - F_c$, $2F_o - F_c$, and omit difference electron density maps were calculated in the region of residue 52 which allowed placement of the substituted isoleucine side chain originally left out of the refinement model. Subsequent positional and thermal factor refinement, followed by a round of simulated annealing refinement (Brunger, 1990), was performed. At this stage further $F_o - F_c$, $2F_o - F_c$ difference electron density maps were calculated, along with a complete set of omit maps in which 10 amino acids were removed sequentially over the entire course of all 112 amino acids in the polypeptide chain. In this manner manual fitting was accomplished, particularly of surface side chains and of the N-terminal six residues which are substantially disordered in electron density maps. This refitting process was followed by further positional and thermal factor refinement to optimize refit sections of polypeptide chain.

Final structural refinement was carried out using a restrained parameter least-squares approach with PROLSQ (Hendrickson, 1985). This involved additional alternating cycles of refinement and manual adjustments based on omit and difference electron density maps. As part of this process, an extensive search for bound water molecules was conducted using the ASIR method (Tong et al., 1994), with subsequent manual verification of the positions identified. All water molecules were refined as neutral oxygen atoms having full occupancy and only those refining to thermal factors smaller than 75 Å^2 were retained in subsequent refinements. In this way a total of 116 water molecules were identified, along with one sulfate ion.

At the end of refinement the crystallographic R factor was 16.2%, and a summary of other refinement results is

Table 2: Stereochemistry of Refined N52I Yeast Iso-2 Cytochrome *c*

stereochemical parameter	rms deviation from ideal values	restraint weight
distances (Å)		
bond (1−2)	0.020	0.016
angle (1−3)	0.036	0.022
planar (1−4)	0.054	0.050
planar restraints (Å)	0.011	0.010
chiral volumes (Å^3)	0.129	0.080
nonbonded contacts (Å)[a]		
single torsion	0.174	0.140
multiple torsion	0.136	0.140
possible hydrogen bond	0.133	0.140
torsion angles (deg)		
planar (0° or 180°)	2.2	3.0
staggered (±60°, 180°)	18.0	12.0
orthonormal (±90°)	18.0	10.0

[a] The rms deviation from ideality for this class of restraint incorporates a reduction of 0.20 Å from the radius of each atom involved in a contact.

presented in Table 1. Table 2 provides an analysis of the stereochemistry of the refined N52I iso-2 cytochrome *c* structure and the restraint weights used. An estimate of 0.16 Å can be made for the overall coordinate error of the current structure based on a Luzzati plot analysis (Luzzati, 1952).

Differential Scanning Calorimetry. Protein samples were prepared by dissolving the lyophilized protein at a concentration of 40 mg mL^{-1} in 4 M guanidine hydrochloride and 0.1 M sodium phosphate, pH 6.0, and heating to 60 °C for 10 min. This treatment is believed to disrupt any aggregated forms caused by lyophilization. To prepare fully oxidized samples, 5−10 mg of solid potassium ferricyanide (Sigma) were added to a 2 mL protein solution. The oxidized protein solutions were passed over a 20 × 2.5 cm G-25 Sephadex column (Pharmacia) that had been washed with four column volumes of 0.05 M sodium phosphate, pH 7.2.

The reversibility of the thermal unfolding transition for the reduced protein was improved by an additional purification step to remove protein that was misfolded or dimerized. This was carried out by loading the protein onto a 50 × 1.0 cm Biorex-70 (Bio-Rad) column equilibrated with 0.05 M sodium phosphate, pH 7.2, and eluting with a linear salt gradient of 0.2−0.8 M NaCl. The major fraction of protein was collected and dialyzed with three buffer changes into 0.1 M ionic strength buffer, pH 6.0. The dialysis buffer was prepared by adding sufficient sodium phosphate to a 0.05 M KCl solution to give an ionic strength of 0.1 M, at a final pH of 6.0.

Scanning Calorimetry: Data Collection and Analysis. Differential scanning calorimetry (DSC)[1] was performed using a MicroCal MC2 differential scanning calorimeter (MicroCal Inc., Northhampton, MA). Prior to filling the calorimeter cells, the final dialysis buffer and protein samples were filtered through a 0.2 μm filter and degassed. Before measuring the temperature dependence of the heat capacity for the oxidized protein solutions, scans were performed with buffer in both the reference and sample cells to determine the instrumental baseline. After obtaining baseline scans, fresh buffer was added to the reference cell and the protein solution added to the sample cell. A Hewlett-Packard 8452A diode array spectrophotometer was used to determine the protein concentrations by measuring the absorbance at 410 nm of the protein solution added to the DSC sample cell. The molar extinction coefficient was assumed to be $\epsilon_{410} = 104 \times 10^3$ M^{-1} cm^{-1} (Liggins et al., 1994; Margoliash & Frohwirt, 1959) for both oxidized and reduced protein samples.

Additional steps were needed for sample preparation and calorimetry measurements on reduced protein samples. The buffer and protein solutions were prepared by sealing the buffer and protein samples in tubes and degassing on a vacuum line. After degassing, dry nitrogen was bubbled through the buffer for 30 min. To avoid surface denaturation of the protein samples, nitrogen gas bubbling was not carried out on the protein solutions. Instead, dry nitrogen gas was passed over the protein solution with continuous stirring. Degassing and nitrogen purging of the protein solutions were carried out a total of three times. After degassing and nitrogen purging, the protein samples were reduced by dissolving 20 mg of sodium dithionite in 1.0 mL of degassed, nitrogen-bubbled buffer and adding 53 μL of the dithionite solution to a 3.0 mL solution of cytochrome *c*. The DSC cells were flushed with dry nitrogen prior to filling with buffer and protein solutions. Instrumental baseline scans with buffer solutions in both cells were carried out in a manner similar to that described for baseline scans for oxidized cytochrome *c* samples. To ensure that the buffer baselines would match the conditions of sample scans, 53 μL of the dithionite solution was added to the sample cell buffer, but not to the reference cell buffer.

The reversibility of the thermal unfolding transitions was measured by performing 3−4 repetitive scans on each protein sample. The buffer baseline was subtracted, and the specific heat capacities were corrected for the partial specific volume of the protein (Privalov & Potekhin, 1986). Partial specific volumes at 25 °C for iso-2 and N52I iso-2 were calculated to be 0.723 and 0.725 cm^3/g, respectively, as described (Makhatadze et al., 1990). The reversibility of the transition was determined as the ratio of the transitional heat for a given thermal scan divided by the area of the immediately preceding scan. The transitional heats were measured by integrating the area between the total heat capacity curve and the progress baseline determined from the heat capacities of the fully folded and fully unfolded proteins. The pretransition and posttransition baselines were often better after the first scan of a given sample. Specific heat capacities were converted to molar heat capacities by dividing by the protein concentration. The protein concentrations for all scans other than the first scan for a given sample were corrected for losses from irreversible unfolding. In general, the thermodynamic parameters obtained from repeated scans of a given sample were in excellent agreement with those obtained from the first scan of the same sample. Reversibility for unfolding of the oxidized proteins was 90−95%. Reversibility of unfolding of the reduced proteins was 70−80% for the first scan. In the first thermal scan of a reduced protein sample, a small amount of material became oxidized (20−30%) and was detected in subsequent thermal scans as a minor transition with the T_m of the oxidized protein. With the exception of the first scan for the reduced protein

[1] Abbreviations: DTT, dithiothreitol; SDS, sodium dodecyl sulfate; THAM, Tris hydroxymethylaminomethane; Gdn·HCl, guanidine hydrochloride; SDS−PAGE, polyacrylamide gel electrophoresis in the presence of sodium dodecyl sulfate; DSC, differential scanning calorimetry; SCE, standard calomel electrode; SHE, standard hydrogen electrode; E_m, midpoint reduction potential.

samples, the percent reversibility was independent of the number of times the sample had been thermally unfolded, and the minor (oxidized protein) transition increased only slightly in area (2−5%) on each subsequent scan. The transitional enthalpy, ΔH_m, was determined by fitting the temperature dependence of the molar heat capacity, $C_P(T)$, to a two-state model with an adjustable $\Delta H^{vH}/\Delta H^{cal}$ value and a temperature-dependent ΔC_P (Liggins et al., 1994).

Direct Electrochemistry. The lyophilized proteins were dissolved in 20 mM sodium phosphate buffer (pH 7.2) and converted to the ferricytochrome *c* by addition of a slight excess of a buffered Co(dipicolinate)$_2$NH$_4$ solution. The resulting solution was clarified by centrifugation, and any soluble, aggregated cytochrome *c* was removed by cation exchange chromatography with a Pharmacia Mono S HR 10/10 column (Rafferty et al., 1990). Samples of the purified protein were exchanged into the buffer used for the electrochemical measurements by repeated concentration and dilution by means of centrifugal ultrafiltration (using Centricon 10 units; Amicon). The protein concentrations used for electrochemical measurements were between 0.2 and 0.4 mM.

Cyclic voltammetry was performed with a two compartment glass cell equipped with a calomel reference electrode (Radiometer K401) and a modified gold electrode as described previously (Rafferty et al., 1990). Electrode potentials were controlled with a Ursar Electronic potentiostat, and the current output was recorded with a Kipp and Zonnen BD90 X-Y recorder. The temperature of the sample was controlled by immersing the sample cell in a thermostated water bath. Midpoint potentials were determined from steady-state voltammograms recorded at a sweep rate of 20 mV s^{-1}, and reduction potentials were converted to the hydrogen scale (SHE) as described by Dutton (1978). Errors in midpoint potentials are estimated to be ±2 mV. The temperature dependence of the midpoint potential is obtained by fitting the data to a linear function of the form: $E_m(T) = [\partial E_m/\partial T]T + E_m(0)$, where the temperature is given in degrees Celcius. Errors in the parameters, $[\partial E_m/\partial T]$ and $E_m(0)$, are obtained from the statistical errors of the fit. The temperature dependence of the free energy of electron binding, $\Delta G_N^{redox}(T)$, is obtained using eq 10. The errors in $\Delta G_N^{redox}(T)$, estimated to be ±50 cal mol^{-1}, are calculated from errors in $E_m(T)$.

Isothermal Thermodynamic Functions. The temperature dependence of $E_m(T)$ for cytochrome *c* was determined by nonisothermal cyclic voltammetry in which the temperature of the protein solution was varied and the temperature of the reference electrode was maintained at $T_{ref} = 25$ °C. Thus, the values of $E_m(T)$ and resulting thermodynamic parameters are those of a nonisothermal oxidation−reduction couple with the initial state of the system at one temperature and the final state at another temperature. To facilitate comparison of thermodynamic properties of the oxidation−reduction reactions to the protein unfolding reactions, thermodynamic relationships are derived that relate the isothermal thermodynamic properties of the oxidation−reduction reactions to (nonisothermal) measurements of the electrochemical potentials.

The half-reaction for the standard hydrogen electrode (SHE) and the corresponding free energy function are

$$(1/2)H_2 = H^+ + e^- \quad (1A)$$

$$\Delta G_H = \Delta H_H - T\Delta S_H \quad (1B)$$

The cytochrome *c* reduction half-reaction and the free energy function are

$$\text{cyt(ox)} + e^- = \text{cyt(red)} \quad (2A)$$

$$\Delta G_{cyt} = \Delta H_{cyt} - T\Delta S_{cyt} \quad (2B)$$

In eq 2 e^- is an electron and cyt(ox) and cyt(red) are the oxidized and reduced forms of cytochrome *c*, respectively.

The complete oxidation−reduction reaction is

$$(1/2)H_2 + \text{cyt(ox)} = H^+ + \text{cyt(red)} \quad (3A)$$

The free energy function for the complete reaction measured under nonisothermal conditions is

$$\begin{aligned}\Delta G_{ni}(T) &= \Delta G_{cyt}(T) + \Delta G_H(T_{ref}) \\ &= [\Delta H_{cyt} + \Delta H_H] - T_{ref}\Delta S_H - T\Delta S_{cyt}\end{aligned} \quad (3B)$$

where the subscript "ni" indicates that the two half-reactions occur at different temperatures (nonisothermal).

The free energy function for the complete reaction measured under isothermal conditions is

$$\begin{aligned}\Delta G(T) &= \Delta G_{cyt}(T) + \Delta G_H(T) \\ &= [\Delta H_{cyt} + \Delta H_H] - T[\Delta S_{cyt} + \Delta S_H]\end{aligned} \quad (3C)$$

The relationship between the nonisothermal free energies and the reduction potentials is

$$\Delta G_{ni}(T) = -nFE_m(T) \quad (4)$$

where $F = 23.06$ cal mol^{-1} mV^{-1} is Faraday's constant, $n = 1$ is the number of electrons in the reaction, and $E_m(T)$ is the midpoint reduction potential in millivolts. In eq 4 the cytochrome *c* reduction half-reaction (eq 2A) takes place at temperature *T*, while the reference half-reaction (eq 1A) occurs at temperature T_{ref}.

Taking the temperature derivatives of eqs 3B and 4 and equating the results gives

$$\Delta S_{cyt} = nF(\partial E_m/\partial T) \quad (5)$$

Thus, ΔS_{cyt}, the entropy of the cytochrome *c* reduction half-reaction, can be obtained from the slope of a plot of the (nonisothermal) midpoint potential $E_m(T)$ vs *T*.

By convention the free energy change for the hydrogen electrode half-reaction is zero at $T = T_{ref} = 25$ °C:

$$\Delta G_H(T_{ref} = 25\ °C) = 0 \quad (6)$$

Inserting eq 6 into eq 1B gives

$$\Delta H_H = T_{ref}\Delta S_H \quad (7)$$

Inserting eq 6 into eq 3B at $T = T_{ref}$ gives

$$\Delta G_{ni}(T_{ref}) = \Delta H_{cyt} - T_{ref}\Delta S_{cyt} \quad (8)$$

Inserting eqs 4 and 5 into eq 8 at $T = T_{ref}$ and solving for ΔH_{cyt} gives

$$\Delta H_{cyt} = -nFE_m(T_{ref}) + T_{ref}nF(\partial E_m/\partial T) \quad (9)$$

Inserting eqs 5, 7, and 9 into eq 3C gives

$$\Delta G(T) = [-nFE_m(T_{ref}) + T_{ref}nF(\partial E_m/\partial T) + T_{ref}\Delta S_H] - T[nF(\partial E_m/\partial T) + \Delta S_H] \quad (10)$$

Equation 10 gives the free energy change for the isothermal oxidation−reduction reaction in terms of nonisothermal values of the midpoint potential, E_m, and the entropy change for the hydrogen electrode half-reaction. Inspection of eq 10 gives the enthalpy change, ΔH, and the entropy change, ΔS, for the total (isothermal) oxidation−reduction reaction:

$$\Delta H = -nFE_m(T_{ref}) + T_{ref}nF(\partial E_m/\partial T) + T_{ref}\Delta S_H \quad (11)$$

$$\Delta S = nF(\partial E_m/\partial T) + \Delta S_H \quad (12)$$

Using the practical entropy scale, the entropy change for the hydrogen electrode half-reaction is $\Delta S_H = -15.6$ cal mol^{-1} K^{-1} (Hanania et al., 1967; Taniguchi et al., 1980). Use of the practical entropy convention has been shown to give good agreement between thermodynamic parameters obtained from nonisothermal and isothermal reduction potential measurements (Taniguchi et al., 1980). Equation 10 is used to obtain $\Delta G_N^{redox}(T)$ in Figure 4B and, together with ΔG_{ox}^U and ΔG_{red}^U, to calculate ΔG_U^{redox}(T) in Figure 8. $\Delta G_N^{redox}(T)$ is the free energy function describing the temperature dependence of electron binding to the folded protein, and $\Delta G_U^{redox}(T)$ is the corresponding free energy function for electron binding to the unfolded protein. ΔG_{ox}^U and ΔG_{red}^U are the free energy functions describing the temperature dependence of unfolding of the oxidized and reduced forms of cytochrome *c*, respectively. Equations 10−12 are used to calculate the thermodynamic quantities for the complete oxidation−reduction reaction listed in Table 5. Equation 5 is used to calculate ΔS_{cyt} in Table 5.

RESULTS

Heat Capacity Measurements of Oxidized and Reduced Proteins. The temperature dependence of the molar heat capacity, $C_P(T)$, is given for the oxidized and reduced forms of iso-2 and N52I iso-2 in Figure 1. The C_P vs T curves were fit to a two-state unfolding transition with variable H^{vH}/H^{cal} value and a temperature-dependent ΔC_P (Connelly et al., 1991; Kitamura & Sturtevant, 1989; Liggins et al., 1994; Sturtevant, 1987). The thermodynamic parameters describing the thermal transitions, T_m, ΔH_m, ΔS_m, are given in Table 3. The reference temperatures for the thermodynamic quantities given in Table 3 are the midpoints of the thermal transitions (T_m) which differ for each protein and which depend on the oxidation state of the protein. Since the reference temperatures differ, the thermodynamic parameters given in Table 3 for different proteins, or different oxidation states of the same protein, should not be compared directly. Note that the values for $\Delta H^{vH}/\Delta H^{cal}$ are significantly greater than unity, suggesting that the transition may be complicated by partial association of the unfolded protein. This deviation from simple two-state behavior has been described previously (Liggins et al., 1994) and indicates that care should be taken in comparing thermodynamic quantities obtained at significantly different protein concentrations.

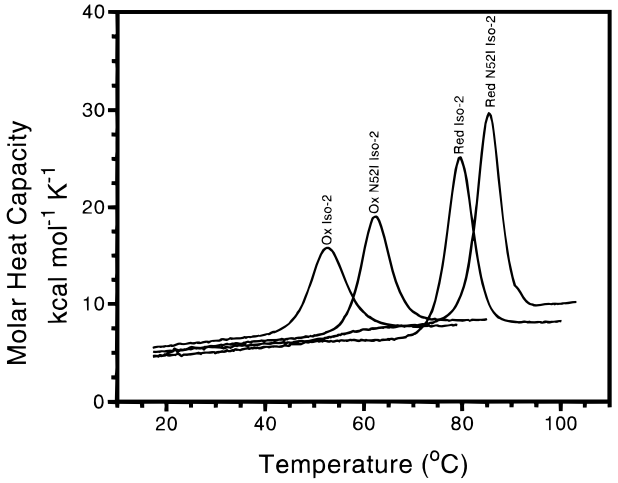

FIGURE 1: Molar heat capacity, C_P, vs temperature for oxidized and reduced forms of iso-2, and the mutant protein, N52I iso-2. The particular variant (iso-2 or N52I iso-2) and oxidation state are indicated near the heat capacity maximum of each thermal scan. The protein concentrations are between 150 and 200 μM in a 0.1 M ionic strength buffer containing 0.05 M KCl and sodium phosphate, pH 6.0. The temperature is increased at a scan rate of 1.5 °C/minute.

Estimation of ΔC_P. A meaningful comparison of the thermodynamic quantities for different proteins requires that they be compared at the same reference temperature. In comparing the stabilities of mutant and normal proteins, the reference temperature is usually chosen to be the midpoint of the thermal unfolding transition (T_m) for the normal protein (Schellman, 1987). Thermal unfolding of proteins involves a large positive change in heat capacity, ΔC_P, so the transitional enthalpies and entropies for protein unfolding are strong functions of temperature. To compare the transitional enthalpies and entropies of unfolding for different proteins at a common temperature, ΔC_P must be determined. The standard means of measuring ΔC_P is by varying pH to shift the transition midpoint for unfolding and plotting the transitional enthalpy vs T_m. ΔC_P is taken to be the slope of the plot of ΔH_m vs T_m. Alternatively, ΔC_P for iso-2 may be estimated from plots of ΔH_m vs T_m in which mutational perturbation or changes in oxidation state (Table 3) are used to shift T_m. Shown in Figure 2 is a plot of ΔH_m vs T_m for the data from Table 3 for unfolding of oxidized and reduced iso-2, and oxidized and reduced N52I iso-2. Superimposed on the data from Table 3 are data for iso-2 obtained previously by the more traditional method of varying pH (Liggins et al., 1994). The linear least-squares fit of all the data yields a value for $\Delta C_P = 1.58 \pm 0.07$ kcal mol^{-1} K^{-1}, where the errors are the statistical errors in the slope obtained from fitting the data to a straight line. The previously published value for the ΔC_P of iso-2 was 1.24 kcal mol^{-1} K^{-1}. We feel that 1.58 kcal mol^{-1} K^{-1} is a more reliable value for ΔC_P, because of the good agreement between the present (Table 3) and previous (Liggins et al., 1994) data sets, and the expansion of the temperature range brought about by including the data from Table 3. A linear dependence of ΔH_m on temperature for iso-1 has been reported previously for proteins differing by point mutations (Hickey et al., 1991; Pielak et al., 1995) and in oxidation state (Cohen & Pielak, 1995).

Comparisons of Thermodynamic Parameters at a Common Reference Temperature. Table 4 lists the enthalpy and

Table 3: Thermodynamic Parameters for Protein Unfolding[a]

protein	concentration[b] (mM)	T_m (°C)	ΔH_m (kcal mol^{-1})	ΔS_m (cal mol^{-1} K^{-1})	$\Delta H^{vH}/\Delta H^{cal}$
oxidized iso-2	0.173	52.4	74.2 ± 0.8	228 ± 2	1.21 ± 0.01
oxidized N52I iso-2	0.196	62.3	87.7 ± 1.4	261 ± 3	1.31 ± 0.01
reduced iso-2	0.155	79.4	113.1 ± 2.8	321 ± 4	1.24 ± 0.03
reduced N52I iso-2	0.195	85.3	129.1 ± 1.1	360 ± 3	1.26 ± 0.02

[a] Thermodynamic parameters for iso-2 and N52I iso-2-cytochrome *c* in a 0.1 M ionic strength buffer containing 0.05 M KCl and sodium phosphate, pH 6.0. T_m is the midpoint of the thermal unfolding transition. Errors in T_m are estimated to be ±0.2 °C. ΔH_m is the calorimetric enthalpy (ΔH^{cal}) of the transition determined at T_m. ΔS_m is the entropy of unfolding at T_m, which is determined from $\Delta S_m = \Delta H_m/T_m$ with T_m in K. The quantity $\Delta H^{vH}/\Delta H^{cal}$ is the ratio of two enthalpies: ΔH^{vH} is the van't Hoff enthalpy and $\Delta H^{cal}(T_m) \equiv \Delta H_m$. Errors are estimated from the standard deviation of multiple measurements. [b] Protein concentrations were determined spectrophotometrically using a molar extinction coefficient of 104 mM^{-1} cm^{-1} at 410 nm, an isosbestic point for oxidized and reduced iso-2 cytochrome *c*.

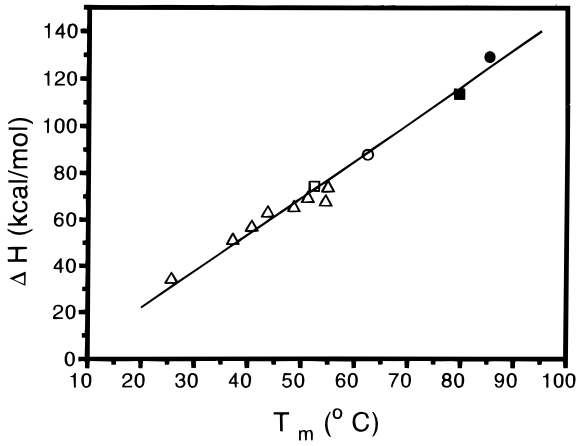

FIGURE 2: Temperature dependence of the transitional enthalpy change on thermal unfolding. The calorimetric enthalpy is plotted vs T_m, the midpoint of the thermal unfolding transition, for the oxidized (open symbols) and reduced (filled symbols) proteins. Data for iso-2 are indicated by squares, while the data for N52I iso-2 are circles. The triangles are data for iso-2 obtained previously by varying the solution pH (Liggins et al., 1994). The solid line drawn through the data is the equation for a line which fits the data best: $\Delta H(T) = [-9.7 \pm 4] + [1.58 \pm 0.07]T$, where the enthalpy is in kcal mol^{-1}, and T is in °C. Errors are estimated from the statistical errors in the slope and intercept obtained on fitting the data to the equation of a straight line. The slope of the plot of ΔH vs temperature gives the transitional change in heat capacity for unfolding, $\Delta C_P = 1.58 \pm 0.07$ kcal mol^{-1} K^{-1}.

Table 4: Thermodynamic Parameters for Unfolding at Reference Temperatures[a]

	T_{ref} (°C)	$\Delta H(T_{ref})$ (kcal mol^{-1})	$\Delta S(T_{ref})$ (cal mol^{-1} K^{-1})	$\Delta G(T_{ref})$ (kcal mol^{-1})
oxidized iso-2	25.0	31 ± 2	89 ± 2	4.4 ± 0.3
oxidized N52I iso-2	25.0	29 ± 3	75 ± 4	6.4 ± 0.6
reduced iso-2	25.0	27 ± 5	50 ± 3	10.5 ± 1.2
reduced N52I iso-2	25.0	34 ± 4	69 ± 3	13.2 ± 1.4
oxidized iso-2	52.4	74 ± 0.8	228 ± 2	(0)
oxidized N52I iso-2	52.4	72 ± 2	214 ± 4	2.4 ± 0.1
reduced iso-2	52.4	70 ± 4	195 ± 3	6.9 ± 0.4
reduced N52I iso-2	52.4	77 ± 3	208 ± 3	9.4 ± 0.5

[a] Thermodynamic parameters are calculated at two reference temperatures, $T_{ref} = 25$ °C, the usual reference temperature, and $T_{ref} = 52.4$ °C, the midpoint for the thermal unfolding transition (T_m) for oxidized iso-2. $\Delta H(T_{ref})$, $\Delta S(T_{ref})$, and $\Delta G(T_{ref})$ were calculated according to Schellman (Becktel & Schellman, 1987; Schellman, 1987) using ΔH_m, and ΔS_m values from Table 3 and $\Delta C_P = 1.58 \pm 0.07$ kcal mol^{-1} K^{-1}.

entropy of unfolding at reference temperatures of $T = 52.4$ °C, the T_m of oxidized iso-2, and at $T = 25$ °C. Compared in this manner, there are no significant differences in the values of $\Delta H(T_{ref})$ for the different proteins regardless of oxidation state or the nature of the amino acid residue at

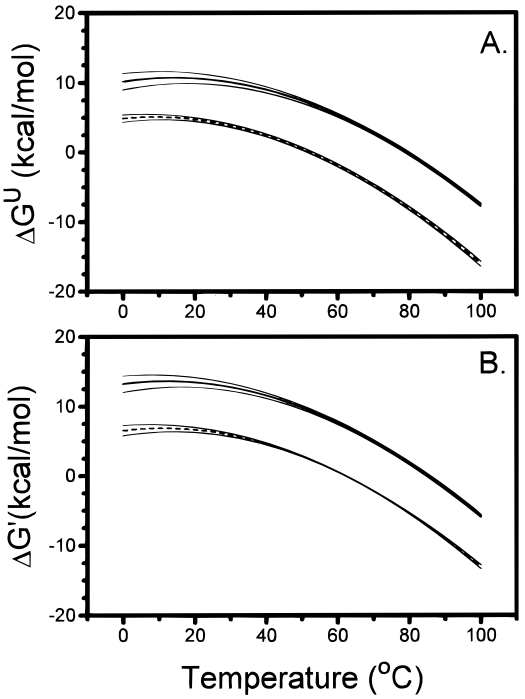

FIGURE 3: Temperature dependence of the free energy of unfolding for the oxidized and reduced forms of iso-2 (A) and N52I iso-2 (B). The heavy solid lines are for unfolding of the reduced forms of the proteins, while the heavy dashed lines are for unfolding of the oxidized forms. The thin lines plotted above and below the free energy curves are estimated error limits for the free energies as determined by eq 14. The free energy functions are obtained from eq 13 using the parameters given in Table 3.

position 52. The similar values for $\Delta H(T_{ref})$ are a necessary consequence of the assumption used to estimate ΔC_P: the dependence of ΔH on temperature for the different proteins and different oxidation states (Table 3) is described by the same linear function (Figure 2). Also given in Table 4 are the free energies of unfolding at the reference temperatures, $\Delta G(T_{ref})$. The values of $\Delta G(T_{ref})$ are much more accurate at $T_{ref} = 52.4$ °C where free energy changes are measured relative to the free energy of unfolding of oxidized iso-2. At 52.4 °C the mutational effects and oxidation−reduction effects on stability are additive. Reduction of iso-2 or N52I iso-2 leads to proteins that are 6.9−7.0 kcal mol^{-1} more stable. Similarly, the N52I mutation increases stability by 2.4−2.5 kcal mol^{-1} in oxidized and reduced forms of the protein. The enhanced stability resulting from heme reduction is a consequence of a smaller ΔS of unfolding for the more stable reduced proteins. Smaller values of ΔS might arise from oxidation−reduction-induced changes in a variety of factors such as the conformational entropies or solvation entropies of the folded or unfolded proteins. Studies of the

stabilities of the oxidized and reduced forms of iso-1 cytochrome *c* also show that the stability differences arise entirely from differences in the transitional entropies (Cohen & Pielak, 1995). Changes in stability resulting from the N52I mutation are too small to be certain whether the mutation-induced stability increase is due to changes in the unfolding entropy, the unfolding enthalpy, or both.

Figure 3 shows plots of the free energy of unfolding, $\Delta G(T)$, versus temperature for the oxidized and reduced forms of iso-2 (Figure 3A) and the oxidized and reduced forms of N52I iso-2 (Figure 3B). $\Delta G(T)$ is calculated from

$$\Delta G(T) = \Delta H_m - T\Delta S_m + \Delta C_P[T - T_m - T\ln(T/T_m)] \quad (13)$$

using the thermodynamic parameters of Table 3 and Figure 2, where T is the temperature in Kelvin. The differences in the free energy of unfolding between the reduced and oxidized forms are largely independent of temperature for iso-2 (Figure 3A) and for N52I iso-2 (Figure 3B).

The propagation of error from the thermodynamic parameters on the right-hand side of eq 13 (Tables 3 and 4; Figure 2) to the free energy of unfolding were calculated using the following formula (Bevington, 1969):

$$\lambda_{\Delta G} = \left[\sum_{x=1}^{N}\left(\frac{\partial \Delta G}{\partial x}\right)^2(\lambda_x)^2\right]^{1/2} \quad (14)$$

where $\lambda_{\Delta G}$ is the (propagated) root mean square error in the free energy of unfolding, and the λ_x are the root mean square errors in the thermodynamic parameters from which ΔG is calculated. The λ_x are taken to be equal to the standard deviations of multiple measurements of the thermodynamic quantities. The summation is carried out for x equal to each of the thermodynamic parameters used to calculate ΔG (i.e., ΔH_m, ΔS_m, T_m, and ΔC_P). The error estimates show that stability comparisons are much more accurate for temperatures near the unfolding transition zones where the data are collected than for lower temperatures. Error estimates of the type shown in Figure 3 are crucial in assessing the significance of apparent stability differences.

Oxidation−Reduction Potentials of the Proteins. The temperature dependence of the midpoint reduction potentials (E_m) for iso-2 and N52I iso-2 are given in Figure 4A. In Figure 4B the data have been converted to electron binding free energies, ΔG_N^{redox}, which are plotted versus temperature. The thermodynamic parameters that describe the dependence of the electron binding free energy on temperature are listed in Table 5 for two reference temperatures. Values are given at 25 °C, the usual standard temperature, but values are also listed for $T = 52.4$ °C, the midpoint of the thermal unfolding transition for oxidized iso-2. Since ΔC_P for electron binding is assumed to be zero, the enthalpy and entropy of electron binding are the same for both reference temperatures.

The N52I mutation decreases the electron binding affinity (Figure 4). The magnitude of the difference in the free energy of binding decreases by 14−16% (0.9−1.1 kcal/mol) over the temperature range investigated, such that the effect of the N52I mutation is slightly smaller at high temperatures. The data for both iso-2 and N52I iso-2 are well described by least-squares fits of the data to the equation for a line, supporting the assumption that $\Delta C_P = 0$ for electron binding.

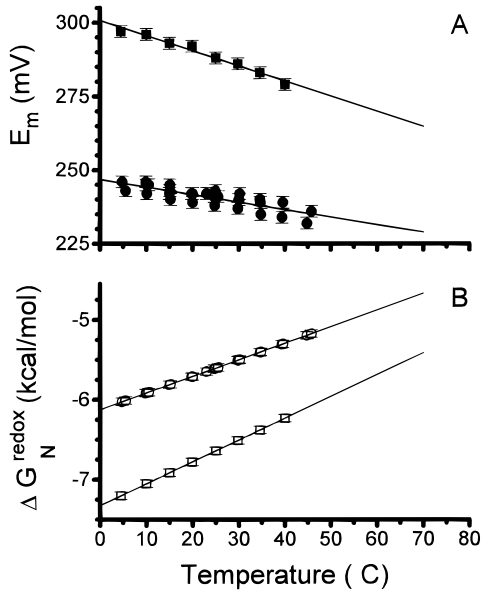

FIGURE 4: Temperature dependence of the midpoint potential (A) and free energy of electron binding (B) for iso-2 (squares) and N52I iso-2 (circles). The solid lines are the least-squares fits of the data to the equation for a line. The midpoint potentials (mV) as a function of the temperature, T (°C), are given by $E_m(T) = [-0.51 \pm 0.03]T + [301 \pm 1]$ for iso-2 and $E_m(T) = [-0.25 \pm 0.03]T + [247 \pm 1]$ for N52I iso-2. Errors in values of E_m are estimated to be ±2 mV. Note that, for temperatures other than 25 °C, $E_m(T)$ is a nonisothermal quantity. This is because the voltammetry measurements are made with the reference half-reaction at 25 °C while the temperature of the cytochrome *c* reduction half reaction is varied. In panel B the temperature dependence of the free energy for electron binding relative to a standard hydrogen electrode is given for the overall isothermal oxidation−reduction reaction. The isothermal free energy of electron binding, $\Delta G^{redox}{}_N$, is obtained from eq 10 in Materials and Methods. Errors in $\Delta G^{redox}{}_N$ and $\Delta G'^{redox}{}_N$ of ±50 cal mol^{-1} are estimated from the error in E_m.

Direct electrochemistry of unfolded cytochrome *c* at elevated temperatures resulted in irreversible behavior that is presumably related to complex linkage between the protein conformational state and the oxidation state of the heme iron. We suggest that this linkage persists because the experimentally accessible temperatures for these experiments with the equipment available to us are insufficient to unfold the cytochrome *c* completely in both oxidation states. Consequently, meaningful measurements of the reduction potential of the thermally unfolded protein could not be obtained in the present study.

Structural Analyses of N52I Iso-2 Cytochrome c. To allow for a comprehensive analysis of the structural effects of the N52I mutation in yeast iso-2 cytochrome *c*, the coordinate set determined for this protein was superimposed on that of the wild type protein using a least-squares procedure involving all main chain and heme atoms. As can be seen in Figure 5, this comparison shows the overall polypeptide chain fold is unaffected by the substitution of isoleucine for asparagine at position 52. The rms deviations for main chain and side chain atoms (excluding residues −9 to −3) between these two structures are 0.28 and 0.60 Å, respectively. Only one region of polypeptide chain, involving residues −9 to −3, has substantially different conformations between the N52I mutant and wild type proteins. However, these residues are disordered in electron density maps of both proteins, and therefore the differing conformations observed undoubtedly reflect alternative fits to the same poorly resolved electron

Table 5: Electrochemical Properties of Iso-2 and N52I Iso-2 Cytochrome *c*[a]

	T_{ref} (°C)	$E_m(T_{ref})$ (mV vs SHE)	$\Delta G(T_{ref})$ (kcal mol^{-1})	$\Delta H(T_{ref})$ (kcal mol^{-1})	$\Delta S(T_{ref})$ (cal mol^{-1} K^{-1})	$\Delta S_{cyt}(T_{ref})$ (cal mol^{-1} K^{-1})
iso-2	25	288 ± 2	−6.6 ± 0.1	−14.8 ± 0.3	−27.4 ± 0.7	−11.8 ± 0.7
N52I iso-2	25	243 ± 2	−5.6 ± 0.1	−11.8 ± 0.2	−20.8 ± 0.4	−5.2 ± 0.4
unfolded iso-2	25	24 ± 52	−0.6 ± 1.2	−18.5 ± 5	−60.4 ± 4	−44.8 ± 4
unfolded N52I iso-2	25	−55 ± 65	1.3 ± 1.5	−6.8 ± 5	−26.8 ± 5	−11.2 ± 5
iso-2	52.4	274 ± 2	−5.9 ± 0.1	−14.8 ± 0.3	−27.4 ± 0.7	−11.8 ± 0.7
N52I iso-2	52.4	233 ± 2	−5.0 ± 0.1	−11.8 ± 0.2	−20.8 ± 0.4	−5.2 ± 0.4
unfolded iso-2	52.4	−29 ± 17	1.1 ± 0.4	−18.6 ± 3	−60.4 ± 4	−44.8 ± 4
unfolded N52I iso-2	52.4	−68 ± 17	2.0 ± 0.4	−6.8 ± 4	−26.8 ± 5	−11.2 ± 5

[a] The electrochemical properties for iso-2 and N52I iso-2 cytochrome *c* in a 0.1 M ionic strength buffer containing 0.05 M KCl and sodium phosphate, pH 6.0. $E_m(T_{ref})$ is the midpoint potential of the voltammogram at $T = T_{ref}$. $\Delta H(T_{ref})$, $\Delta S(T_{ref})$, and $\Delta G(T_{ref})$ are the changes in enthalpy, entropy, and free energy for the overall electron binding reaction at $T = T_{ref}$. ΔS_{cyt} is the entropy of the cytochrome *c* reduction half-reaction which is given by eq 5 in Materials and Methods. The thermodynamic parameters associated with electron binding are given at two reference temperatures: $T_{ref} = 25$ °C, a conventional reference temperature, and $T_{ref} = 52.4$ °C, the T_m for thermal unfolding of oxidized iso-2. The inclusion of values for 52.4 °C allows comparison to the thermodynamic quantities listed in Table 4 for the thermal unfolding transitions. Note that the values of $\Delta H(T_{ref})$, $\Delta S(T_{ref})$, and $\Delta S_{cyt}(T_{ref})$ are the same at both reference temperatures since these parameters are temperature independent. The values for $E_m(T_{ref})$ and $\Delta G(T_{ref})$ for folded proteins are obtained by evaluating the functions obtained from fits to the data in Figure 4. $E_m(T_{ref})$ and $\Delta G(T_{ref})$ for unfolded proteins are obtained by use of a thermodynamic cycle (Figure 7) and thermodynamic parameters given in Tables 4 and 5. At temperatures other than 25 °C, $E_m(T)$ is a nonisothermal quantity. This is because the voltammetry measurements are made with the reference half-reaction at 25 °C while the temperature of the cytochrome *c* reduction half-reaction is varied. All other quantities are for isothermal reactions.

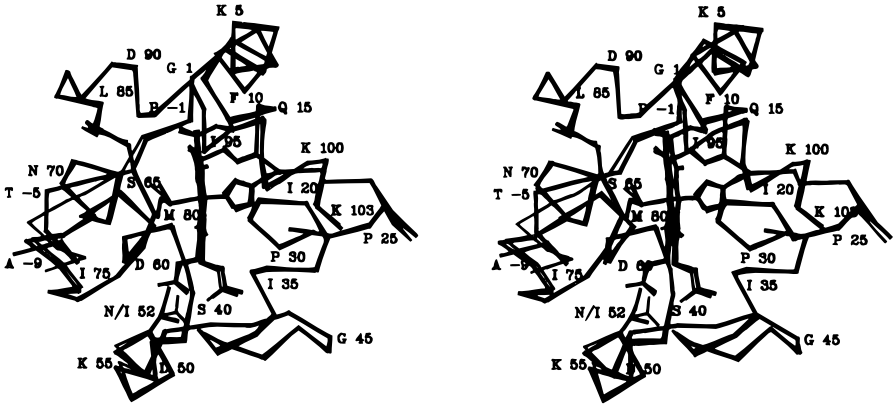

FIGURE 5: Stereodrawing of the α-carbon backbone of the reduced structures of N52I (thick lines) and wild type (thin lines) yeast iso-2 cytochromes *c*. The heme group has also been drawn as well as the two heme ligands, His18 and Met80, and the cysteines 14 and 17, which form thioether bonds to the heme porphyrin ring. In addition, the side chain atoms of residue 52, which is replaced in the mutant protein, is also displayed. To assist interpretation of this drawing, every fifth amino acid along the polypeptide chain has been labeled with its one-letter designation and sequence number. A complete listing of the primary sequence of yeast iso-2 cytochrome *c* can be found in Bushnell et al. (1990), along with a comparison with the sequences of other cytochromes *c* for which structures have been determined.

density, rather than being a consequence of the introduced mutation.

As illustrated in Figure 6, directly in the vicinity of the mutation site the primary consequence of introducing an isoleucine at sequence position 52 is to exclude an internally bound water molecule, Wat106. This water molecule in the wild type protein occupies a central position between Asn52, Tyr67, and Thr78, to all of which it forms hydrogen bond interactions. In the presence of Ile52 there is insufficient space for the normally resident Wat106, and this causes a number of rearrangements of the local hydrogen bond network. One of these is the shift of the side chain of Tyr67 ($\Delta d = 0.72$ Å for side chain atoms) so that this residue now forms a hydrogen bond to Thr78 OG1 ($d = 3.1$Å), while at the same time breaking a hydrogen bond previously made to Met80 SD. The Ile52 side chain also appears to cause a slight displacement in the placement of the propionate A group of the heme (Figure 6). Nonetheless the overall heme geometry remains comparable to that of the wild type protein. With the exception of residues 36−38, the thermal factor profile of atoms over the course of the polypeptide chain also appears to be similar for both the N52I mutant and wild type proteins. For the main chain atoms of residues 36−38 an overall average increase in thermal factors of 7.5 Å^2 is observed in the N52I mutant protein. However, the side chain of Arg38, which interacts with heme propionate A, maintains a mobility comparable to that found in wild type iso-2 cytochrome *c*.

DISCUSSION

Folded Proteins: Correlations between Stability and Structure. Extensive X-ray crystallographic structural studies of reduced and oxidized yeast iso-1 cytochrome *c* (Berghuis & Brayer, 1992) and of the closely related reduced iso-2 cytochrome *c* (Murphy et al., 1992; Murphy, 1993) have allowed for a comprehensive analysis of the effects of oxidation state and the introduction of specific mutants on the stability of these cytochromes *c*. Several features of the less stable oxidized iso-1 protein distinguish it from its more stable reduced form. Among the most striking features, however, is that there are minimal positional changes in the polypeptide chain between oxidation states. An important indicator of similarity in backbone folding is that all main chain to main chain hydrogen bonds are the same in both oxidation states. Changes that do occur are focused in three areas: (1) adjustments to heme structure, (2) movement of

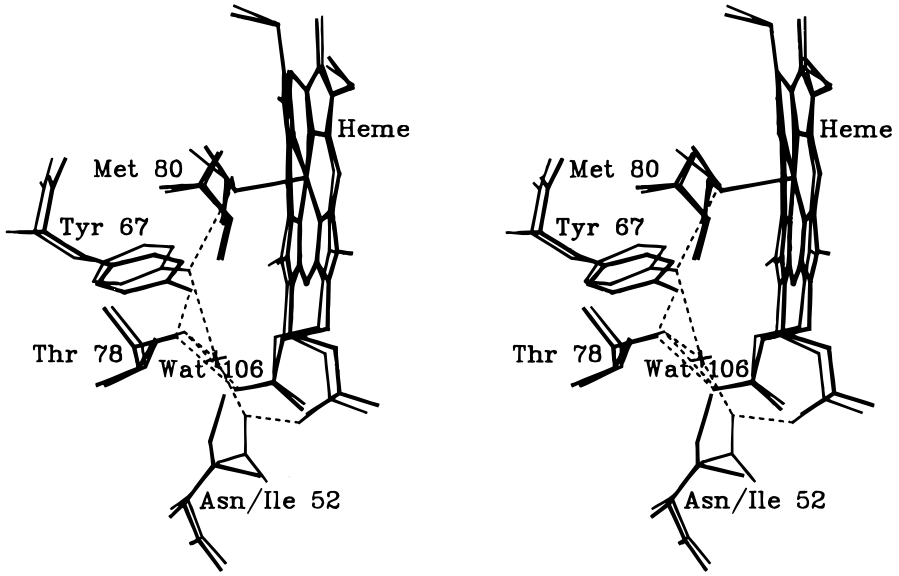

FIGURE 6: Stereodiagram of the region around the N52I mutation site in yeast iso-2 cytochrome *c*. The structure of the N52I mutant protein is shown in thick lines, while wild type yeast iso-2 cytochrome *c* is drawn with thin lines. Hydrogen bonds are indicated by dashed lines. Substitution of isoleucine for asparagine at position 52 results in the removal of the internally bound water, Wat106, and several adjustments in the hydrogen bond network that involved this group. Prominent among these is the formation of a new hydrogen bond between Tyr67 and Thr78 which is made possible by a shift in the side chain of the former residue.

internal water molecules, and (3) shifts in thermal parameters for specific segments of polypeptide chain. Oxidation state dependent changes in heme structure primarily involve the pyrrole A propionate and the associated hydrogen bond to Asn52, which is lost in the oxidized state. However, the largest structural shift occurring between oxidation states involves a conserved internal water molecule, Wat166 (Wat106 in iso-2 cytochrome *c*). In the oxidized state this water molecule moves ~1.7 Å toward the heme iron atom resulting in considerable adjustments to the hydrogen bond network in which it participates with Asn52, Tyr67, and Thr78 (Berghuis et al., 1994). In the oxidized state, three segments of polypeptide chain involving residues 47−59, 65−72, and 81−85 also exhibit increased mobility. The residues most strongly affected in each of these segments are Asn52, Tyr67, and Phe82.

Exactly how oxidation-dependent structural changes result in a dramatic increase in stability of the reduced protein is unclear. In some cases the changes are opposite to what might be expected. For example, increased segmental motion in the oxidized protein might be expected to increase the polypeptide chain entropy of the folded protein and enhance its stability relative to the unfolded form, but exactly the opposite is observed. It seems likely that much of the stability increase in reduced cytochrome *c* is a consequence of increased ligand bond strengths (Komar-Panicucci et al., 1994), but the changes in hydrogen bonding may also play a role.

A central residue in oxidation−reduction-induced structural changes appears to be Asn52. Not surprisingly mutation of this residue has a significant impact on the structural and functional properties of cytochrome *c* (Berghuis et al., 1994; Hickey et al., 1991). The most conspicuous structural change is the loss of the conserved water molecule (Wat166 in iso-1 and Wat106 in iso-2) that undergoes a large oxidation state dependent positional shift (see Figure 6). Associated with the loss of this water molecule is a shift in the position of the side chain of Tyr67 which leads to the breakage of a hydrogen bond formed between Tyr67 OH and the SD side chain atom of the heme ligand Met80. Presumably it is the loss of this hydrogen bond that lowers the midpoint potential of the N52I mutant protein. Tyr67 at its new location is found to form a hydrogen bond with Thr78 OG1. Also absent in the N52I mutant protein are the hydrogen bonds formed by Asn52. This seems to dampen oxidation state dependent conformational changes in the region of the heme propionate A group. A final important influence of the N52I mutation is the absence of increased mobility in the three segments of polypeptide chain earlier identified as undergoing this transition in the oxidized state. Thus the thermal parameter profile for N52I mutant proteins appears to be independent of oxidation state and more like those of the rigid reduced forms of the wild type proteins. As discussed earlier and illustrated in Figures 5 and 6, the structural changes documented for the N52I mutant of iso-2 cytochrome *c* are comparable to those observed for the iso-1 protein in the reduced state. Although it has not proven possible to obtain crystals for structural studies of the oxidized structures of either the wild type iso-2 or the related N52I mutant protein, the close similarity of the corresponding reduced structures of iso-2 and iso-1 cytochromes *c* clearly suggests that comparable changes to those observed for oxidized iso-1 cytochrome *c* will also be observed in the case of the iso-2 proteins. This has been assumed for the purposes of the following discussion.

A surprising consequence of the N52I mutation is that, for a mutation involving a single amino acid change, there is an unusually large enhancement in protein stability. For a reference temperature at the midpoint of the oxidized iso-2 unfolding transition, oxidized N52I iso-2 is 2.4 kcal mol^{-1} more stable than oxidized iso-2. The stability enhancement is essentially the same for reduced N52I iso-2, which is 2.5 kcal mol^{-1} more stable than reduced iso-2 (Table 4). Are there structural differences between N52I iso-2 and iso-2 that explain the stability differences? The differences in hydrogen bonding and segmental motion are among the most likely

structural features that can be expected to alter the thermodynamic properties of unfolding. Replacement of Asn52 by Ile52 removes several hydrogen bonds. Two are lost when the Asn52 side chain is replaced by the non-hydrogen-bonding Ile side chain, and two more hydrogen bonds are lost when Wat106 is displaced. In addition a Tyr 67 OH to Met80 hydrogen bond is replaced by a Tyr 67 OH to Thr 78 OG hydrogen bond. One would have thought that this would result in a significant reduction in stability, perhaps by as much as 5.2 kcal mol^{-1} assuming 1.3 kcal mol^{-1} for each hydrogen bond (Shirley et al., 1992). Unfortunately, the stability change is in the opposite direction than predicted by counting hydrogen bonds. Of course displacement of Wat106 leads to the loss of *intermolecular* hydrogen bonds for which the value of 1.3 kcal mol^{-1} of hydrogen bonds may not apply. The differences in segmental mobility for the different oxidation states might be expected to lead to differences in the configurational entropy of unfolding for the polypeptide chains. Thus, the entropy of unfolding should be greater for the oxidized N52I variants than for the normal isozymes. This is because the segmental motion is reduced in N52I iso-2 compared to iso-2, so the changes in motion on unfolding should be greater. However, the observed entropy changes differ only slightly in the opposite of the expected direction (Table 4). A difference between iso-2 and N52I iso-2 that is in accord with the stability enhancement of N52I iso-2 is the increased hydrophobicity of the Ile side chain over the Asn side chain. Assuming that the N52I mutation results in the introduction of two new -CH- groups, the stability increase would be about 2.6 kcal mol^{-1} [1.3 kcal mol^{-1} of -CH- group (Pace, 1992)]. Nevertheless, the stability gain from enhanced hydrophobicity should be more than offset by the losses in hydrogen bonding. In summary, there is no clear understanding of the enhanced stability of N52I iso-2 in terms of differences in structure of the folded forms of the mutant and wild-type proteins.

Thermally Unfolded Proteins: *Reduction Potential as a Test for Functionally Important Residual Structure.* The simplicity of the function of cytochrome *c* together with a means of measuring the stability of both oxidation states of the native protein provides an efficient test for functionally relevant residual structure in the unfolded protein. The test involves use of a thermodynamic cycle to measure the reduction potential of unfolded cytochrome *c* and comparisons with mutant proteins to assess changes in functionally important residual structure.

Figure 7 gives the thermodynamic cycle relating the thermodynamic stabilities of the folded conformations of the oxidized and reduced native proteins to the free energies of electron binding for the folded and unfolded proteins. Except for the free energy of electron binding for the unfolded protein ($\Delta G^{\text{redox}}{}_{\text{U}}$), all of the free energy functions shown in Figure 7 have been measured. The thermodynamic cycle provides the means of measuring the oxidation−reduction free energy change in the unfolded protein, a property directly related to the function of native, folded cytochrome *c*. Additionally, when applied to both iso-2 and N52I iso-2, the cycle of Figure 7 can be used to test whether the N52I mutation alters the electron binding free energy of the unfolded protein.

The predicted oxidation−reduction free energy change for unfolded iso-2 through the thermodynamic cycle (Figure 7)

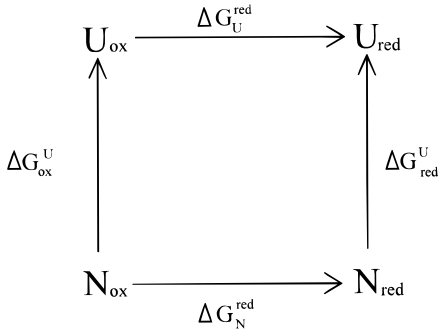

FIGURE 7: Thermodynamic cycle showing the linkage between a functional property, electron binding, and thermal stability of the oxidized and reduced forms of cytochrome *c*. The free energy changes on electron binding are ΔG_N^{red} and ΔG_U^{red}. Free energy changes associated with thermal unfolding are $\Delta G^{U}{}_{ox}$ and $\Delta G^{U}{}_{red}$. Superscripts denote the processes: unfolding, U; electron binding, red. Subscripts reflect the state of the heme: oxidized, ox; reduced, red; or the conformational state of the protein, native, N; unfolded, U.

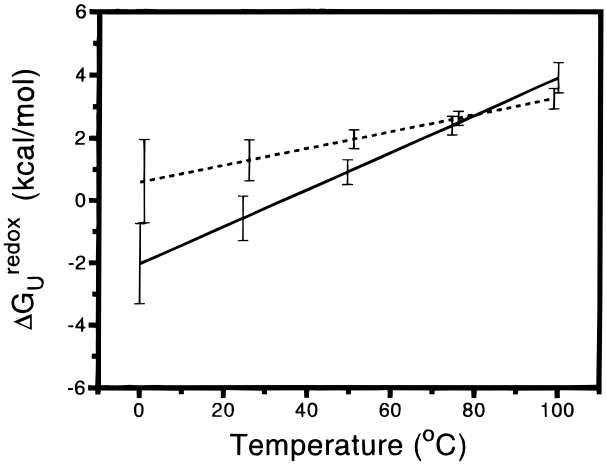

FIGURE 8: Comparison of the reduction potential of thermally unfolded iso-2, $\Delta G^{\text{redox}}{}_{\text{U}}$ (solid line), to the reduction potential of thermally unfolded N52I iso-2, $\Delta G'^{\text{redox}}{}_{\text{U}}$ (dashed line). $\Delta G^{\text{redox}}{}_{\text{U}}$ and $\Delta G'^{\text{redox}}{}_{\text{U}}$ are obtained by summing the free energies around the thermodynamic cycle in Figure 7 (eqs 15 and 16 in text). The difference between the solid and dashed lines measures $|\Delta G^{\text{redox}}{}_{\text{U}} - \Delta G'^{\text{redox}}{}_{\text{U}}|$, the mutation-induced change in the oxidation−reduction free energy of the unfolded proteins. The vertical bars give estimates of the errors.

can be written as follows:

$$\Delta G^{\text{redox}}{}_{\text{U}} = \Delta G^{\text{redox}}{}_{\text{N}} - \Delta G^{\text{U}}{}_{\text{ox}} + \Delta G^{\text{U}}{}_{\text{red}} \qquad (15)$$

Similarly, the predicted oxidation−reduction free energy change for unfolded N52I iso-2 can be written as

$$\Delta G'^{\text{redox}}{}_{\text{U}} = \Delta G'^{\text{redox}}{}_{\text{N}} - \Delta G'^{\text{U}}{}_{\text{ox}} + \Delta G'^{\text{U}}{}_{\text{red}} \qquad (16)$$

where primes are used to denote the free energies for N52I iso-2. All of the quantities on the right-hand sides of eqs 15 and 16 have been determined experimentally, so $\Delta G^{\text{redox}}{}_{\text{U}}$ can be calculated and compared to $\Delta G'^{\text{redox}}{}_{\text{U}}$ (Figure 8). There are no significant differences between $\Delta G^{\text{redox}}{}_{\text{U}}$ and $\Delta G'^{\text{redox}}{}_{\text{U}}$ at higher temperatures (>80 °C). At the reference temperature, 52.4 °C, the difference in the oxidation−reduction free energy change for the two unfolded proteins ($|\Delta G^{\text{redox}}{}_{\text{U}} - \Delta G'^{\text{redox}}{}_{\text{U}}|$) is ∼0.9 kcal mol^{-1}, which is very close to the estimated errors. At lower temperatures the estimated errors grow quickly so differences must be interpreted with caution.

Nevertheless, $\Delta G^{redox}{}_U$ and $\Delta G'^{redox}{}_U$ appear to diverge as the temperature decreases, suggesting that the unfolded proteins contain structure at low temperature sensitive to oxidation state and mutation.

A paper from the McLendon and Sherman laboratories has reported that $\Delta G^{redox}{}_U = \Delta G'^{redox}{}_U$ for analogous iso-1 mutant proteins in the presence of a high concentrations of guanidine hydrochloride (Komar-Panicucci et al., 1994). This result contrasts with the oxidation−reduction free energy differences measured for the thermally unfolded forms of iso-2 and N52I iso-2 in the absence of denaturants. The most likely explanation is that functionally important structural preferences in unfolded proteins are susceptible to high concentrations of protein denaturants. $\Delta G'^{redox}{}_U$ is more likely to differ from $\Delta G^{redox}{}_U$ under conditions more conducive to residual structure formation such as in thermally unfolded cytochrome *c*. Assuming that reduction potential differences between unfolded forms of the two isozymes are negligible, then the electron binding free energies are much more favorable for thermally unfolded cytochrome *c* than for the guanidine hydrochloride unfolded forms. For example, Komar-Panicucci et al. (1994) report that, in the presence of guanidine hydrochloride concentrations equal to or greater than 4.5 M, $E_m = -188$ mv at pH 6, 25 °C for iso-1 and N52I iso-1. This corresponds to a free energy of electron binding $\Delta G^{redox}{}_U = 4.3$ kcal mol^{-1} for the guanidine hydrochloride unfolded forms of iso-1. In contrast, thermally unfolded forms of iso-2 and N52I iso-2 have much more favorable free energies of electron binding: $\Delta G^{redox}{}_U = -0.6 \pm 1.2$ kcal mol^{-1} ($E_m = 24 \pm 52$ mv) for thermally unfolded iso-2; and $\Delta G^{redox}{}_U = 1.3 \pm 1.5$ kcal mol^{-1} ($E_m = -55 \pm 65$ mv) for thermally unfolded N52I iso-2 (Table 5). Also, the electron binding affinity of thermally unfolded iso-2 and N52I iso-2 appears to depend on the presence of the N52I mutation, while the affinity of electron binding is the same for guanidine hydrochloride unfolded iso-1 and N52I iso-1.

Even more striking is the comparison of the E_m values for unfolded iso-2 and N52I iso-2 to those for the heme-containing octapeptide CAQCHTVE. At pH 6, 25 °C unfolded iso-2 has $E_m = +24$ mv, while $E_m = -55$ mv for unfolded N52I iso-2 (Table 5). For the octapeptide (pH 7, 30 °C) $E_m = -210$ mv in the presence of imidazole but increases to −53 mv in the presence of 2 M *N*-acetyl-methionine (Harbury et al., 1965). It is reasonable to assume that the model peptide in the presence of methionine retains histidine as one heme ligand while methionine is the other, i.e., the heme ligation is probably the same as for the folded protein, while the heme environment is that of an unfolded protein. Thus, the thermally unfolded forms of cytochrome *c* have E_m values closer to that of model heme peptides with native-like heme ligands (methionine and histidine) than to model heme peptides with imidazole (histidine) heme ligands. This is despite the fact that unfolded cytochromes *c* at neutral pH are known to have two histidine side chains as heme ligands (Babul & Stellwagen, 1971). Moreover, the $E_m \sim 0$ mv for thermally unfolded isocytochrome *c* is roughly midway between the $E_m = -188$ mv for guanidine hydrochloride unfolded iso-1 (Komar-Panicucci et al., 1994) and $E_m \sim +240-290$ mv for folded iso-2 and N52I iso-2. These observations strongly support the hypothesis that thermally unfolded cytochromes *c* contain reduction potential-modulating structure that is melted out by high denaturant concentrations.

Comparison of Calorimetric and van't Hoff Enthalpies. As reported previously (Liggins et al., 1994) and as shown in Table 3, the quantity $\Delta H^{vH}/\Delta H^{cal}$ is significantly greater than unity. This observation is controversial, at least for iso-1. Values of $\Delta H^{vH}/\Delta H^{cal}$ much closer to 1 have been reported for iso-1 (Betz & Pielak, 1992; Cohen & Pielak, 1995), but we consistently observe values greater than 1 for iso-1 and iso-2. One interpretation of $\Delta H^{vH}/\Delta H^{cal} > 1$ is that unfolding involves intermolecular cooperation (Sturtevant, 1987). We have tested this directly by sedimentation equilibrium and sedimentation velocity both of which indicate a single, low molecular weight species. Unfortunately, the sedimentation equilibrium experiments are complicated by strong polyelectrolyte effects resulting in an apparent molecular weight of less than the formula molecular weight (C. S. Raman, unpublished results). It is not known whether the same polyelectrolyte effects can also affect $\Delta H^{vH}/\Delta H^{cal}$. The value of $\Delta H^{vH}/\Delta H^{cal}$ is known to be (1) independent of temperature, (2) unaffected by low concentrations of protein denaturants, and, in the concentration range needed for accurate determination of the value of $\Delta H^{vH}/\Delta H^{cal}$, (3) independent of protein concentration (Liggins et al., 1994). It is possible that association, if it occurs on unfolding, may contribute to residual structure in the unfolded state. Whatever causes $\Delta H^{vH}/\Delta H^{cal}$ to exceed 1, the value of $\Delta H^{vH}/\Delta H^{cal}$ is similar for unfolding of the oxidized and the reduced proteins (Table 3). This may result in similar effects on $\Delta G^{U}{}_{ox}$ and $\Delta G^{U}{}_{red}$. If so, effects on the values of $\Delta G^{redox}{}_U$ and $\Delta G'^{redox}{}_U$ calculated via the thermodynamic cycle (Figure 7; eqs 15 and 16) may cancel to first order.

Deviations of $\Delta H^{vH}/\Delta H^{cal}$ from unity are not unusual in calorimetric studies of thermal unfolding and have been reported for T4 lysozyme (Kitamura & Sturtevant, 1989), staphylococcal nuclease (Tanaka et al., 1993), and ribonuclease T1 (Hu et al., 1992). For horse cytochrome *c* $\Delta H^{vH}/\Delta H^{cal}$ is slightly less than 1 for measurements between pH 2 and 4.6 (Privalov & Khechinashvili, 1974). Nonnative forms of horse cytochrome *c* are present below pH 5 and have been characterized extensively by calorimetry (Potekhin & Pfeil, 1989). Near neutral pH where horse cytochrome *c* is fully in the native state (i.e., His18 and Met80 as heme ligands), the thermal unfolding transition cannot be analyzed because the protein aggregates irreversibly. In contrast, the thermal unfolding transitions of iso-1 and iso-2 approach full reversibility (>95%) under conditions (pH 6) where the native conformer is the only folded species present (Liggins et al., 1994). Thus, while values of $\Delta H^{vH}/\Delta H^{cal} > 1$ indicate significant deviations from ideality, it is at least possible to measure reversible thermal transitions for unfolding of the forms of iso-1 and iso-2 with native heme ligands.

Guideposts for Protein Folding. An important clue to deciphering the protein folding code is provided by the speed with which polypeptide chains fold to a highly organized, functional form. Folding times of 0.1 s or less imply that the process of folding involves a very small fraction of the potential "random coil" conformations of the polypeptide (Dill, 1985). To occur as fast as it does, folding of small proteins like cytochrome *c* must involve no more than $10^{12}-10^{13}$ conformational states. The "random coil" form of a small 100 residue protein consists of perhaps 10^{50} isoenergetic conformations. Thus folding may involve a reduction in the number of conformations by factors of the

order of 10^{40} or larger (Dill, 1985). The manner in which the enormous number of potential conformations is restricted to a select few is a key question in understanding the mechanism of folding. One proposal is that unfolded proteins may not be as unfolded as supposed (Alexandrescu et al., 1994; Dill & Shortle, 1991; Flanagan et al., 1992; Shortle & Abeygunawardana, 1993; Shortle & Meeker, 1986, 1989). The unfolded polypeptide may contain important pre-existing elements of residual structure which act to guide folding along a productive and highly restricted pathway. While residual structure of any type may be of importance in guiding folding, residual structure imparting limited but detectable levels of function is especially interesting. Functionally relevant residual structure may provide guideposts for directing folding toward a fully functional native conformation. Might not residual function-enhancing interactions in an unfolded protein be a means of initiating the process of folding which, by producing a native protein, maximizes functional interactions? This possibility has been recognized previously (Furie et al., 1974, 1975; Sachs et al., 1972, 1974), but the difficulty of detecting functionally important residual structure has severely limited experimental studies.

CONCLUSIONS

Reversible thermal unfolding transitions have been measured for the oxidized and reduced forms of iso-2 cytochrome *c* and N52I iso-2, a variant form of iso-2 with enhanced stability. In addition, the oxidation−reduction potentials (electron binding) have been measured for the folded proteins. Use of a thermodynamic cycle allows calculation of the free energy of electron binding to the thermally unfolded forms of the proteins. The results show that electron binding to the thermally unfolded proteins is much stronger than expected when compared to model heme−ligand complexes. Also, the N52I mutation weakens electron binding to thermally unfolded N52I iso-2. Taken together, the results suggest that structure in the thermally unfolded proteins enhances electron binding and that the N52I mutation partially disrupts this structure. Both the N52I mutation and electron binding significantly enhance the stability of the folded proteins relative to unfolded forms. Inspection of the high-resolution X-ray structures shows that increased stability of the folded proteins is correlated with modifications in hydrogen bonding involving a conserved water molecule and with changes in the mobility of specific polypeptide chain segments. Nevertheless, there is no obvious structural explanation for the enhanced stability.

ACKNOWLEDGMENT

We thank Susan Weintraub for the electrospray ion mass spectrometry and Guy Guillemette for advice on the site-directed mutagenesis methods. We are grateful to Michael Smith and Jeanette Johnson for providing strains and plasmids and thank Christy MacKinnon for construction of the pEMBLYe30-CYC7 plasmid. C. S. Raman is thanked for assistance in setting up the calorimeter, for help with the data analysis software, and for keeping the calorimeter functioning properly. C. S. Raman is also thanked for the ultrcentrifugation experiments that test for association in the folded and unfolded protein.

REFERENCES

Alexandrescu, A. T., Abeygunawardana, C., & Shortle, D. (1994) *Biochemistry 33*, 1063−1072.
Babul, J., & Stellwagen, E. (1971) *Biopolymers 10*, 2359−2361.
Becktel, W. J., & Schellman, J. A. (1987) *Biopolymers 26*, 1859−1877.
Berghuis, A. M., & Brayer, G. D. (1992) *J. Mol. Biol. 223*, 959−976.
Berghuis, A. M., Guillemette, J. G., McLendon, G., Sherman, F., Smith, M., & Brayer, G. D. (1994) *J. Mol. Biol. 236*, 786−799.
Bernstein, F. C., Koetzle, T. F., Williams, G. J. B., Meyer, E. F. J., Brice, M. D., Rodgers, J. R., Kennard, O., Shimanouchi, T., & Tasumi, M. (1977) *J. Mol. Biol. 112*, 535−542.
Betz, S. F., & Pielak, G. J. (1992) *Biochemistry 31*, 12337−12344.
Bevington, P. R. (1969) *Data Reduction and Error Analysis for the Physical Sciences*, McGraw-Hill Book Company, New York.
Brunger, A. T. (1990) *Acta Crystallogr. Sec. A 46*, 585−593.
Brunger, A. T. (1992) *X-PLOR: A System for X-ray Crystallography and NMR*, Yale University Press, New Haven, CT.
Bushnell, G. W., Louie, G. V., & Brayer, G. D. (1990) *J. Mol. Biol. 214*, 585−595.
Cohen, D. S., & Pielak, G. J. (1995) *J. Am. Chem. Soc. 117*, 1675−1677.
Connelly, P., Ghosaini, L., Hu, C. Q., Kitamura, S., Tanaka, A., & Sturtevant, J. M. (1991) *Biochemistry 30*, 1887−1891.
Creighton, T. E. (1994) in *Mechanisms of Protein Folding* (Pain, R. H., Ed.) pp 1−25, IRL Press at Oxford University Press, Oxford.
Dill, K. (1985) *Biochemistry 24*, 1501−1509.
Dill, K. A., & Shortle, D. (1991) *Annu. Rev. Biochem. 60*, 795−825.
Dutton, P. L. (1978) *Methods Enzymol. 54*, 411−435.
Flanagan, J. M., Kataoka, M., Shortle, D., & Engelman, D. M. (1992) *Proc. Natl. Acad. Sci. U.S.A. 89*, 748−752.
Furie, B., Schechter, A. N., Sachs, D. H., & Anfinsen, C. B. (1974) *Biochemistry 13*, 1561−1566.
Furie, B., Schechter, A. N., Sachs, D. H., & Anfinsen, C. B. (1975) *J. Mol. Biol. 92*, 497−506.
Guillemette, J. G., Barker, P. D., Eltis, L. D., Lo, T. P., Smith, M., Brayer, G. D., & Mauk, A. G. (1994) *Biochimie 76*, 592−604.
Hanania, G. I. H., Irvine, D. H., Eaton, W. A., & George, P. (1967) *J. Phys. Chem. 71*, 2022−2030.
Harbury, H. A., Cronin, J. R., Fanger, M. W., Hettinger, T. P., Murphy, A. J., Meyer, Y. P., & Vinogradov, S. N. (1965) *Proc. Natl. Acad. Sci. U.S.A. 54*, 1658−1664.
Hendrickson, W. A. (1985) *Methods Enzymol. 115 B*, 252−270.
Hickey, D. R., Berghuis, A. M., Lafond, G., Jaeger, J. A., Cardillo, T. S., McLendon, D., Das, G., Sherman, F., Brayer, G. D., & McLendon, G. (1991) *J. Biol. Chem. 266*, 11686−11694.
Higashi, T. (1990) *J. Appl. Crystallogr. 23*, 253−257.
Hu, C. Q., Sturtevant, J. M., Thomson, J. A., Erickson, R. E., & Pace, C. N. (1992) *Biochemistry 31*, 4876−4882.
Inglis, S. C., Guillemette, J. G., Johnson, J. A., & Smith, M. (1991) *Protein Eng. 4*, 569−574.
Kitamura, S., & Sturtevant, J. M. (1989) *Biochemistry 28*, 3788−3792.
Komar-Panicucci, S., Weis, D., Bakker, G., Qiao, T., Sherman, F., & McLendon, G. (1994) *Biochemistry 33*, 10556−10560.
Levinthal, C. (1968) *J. Chim. Phys. 65*, 44.
Liggins, J. R., Sherman, F., Mathews, A. J., & Nall, B. T. (1994) *Biochemistry 33*, 9209−9219.
Lin, T. Y., & Kim, P. S. (1989) *Biochemistry 28*, 5282−5287.
Lin, T. Y., & Kim, P. S. (1991) *Proc. Natl. Acad. Sci. U.S.A. 88*, 10573−10577.
Lu, J., Baase, W. A., Muchmore, D. C., & Dahlquist, F. W. (1992) *Biochemistry 31*, 7766−7772.
Luzzati, V. (1952) *Acta Crystallogr. 5*, 802−810.
Makhatadze, G. I., Medvedkin, V. N., & Privalov, P. L. (1990) *Biopolymers 30*, 1001−1010.
Margoliash, E., & Frohwirt, N. (1959) *Biochem. J. 71*, 570.
Montgomery, D. L., Leung, D. W., Smith, M., Shalit, P., Faye, G., & Hall, B. D. (1980) *Proc. Natl. Acad. Sci. U.S.A. 77*, 541−545.
Murphy, M. E., Nall, B. T., & Brayer, G. D. (1992) *J. Mol. Biol. 227*, 160−176.

Murphy, M. E. P. (1993) Ph.D. Thesis, University of British Columbia, Vancouver, BC.
Nall, B. T., & Landers, T. A. (1981) *Biochemistry 20*, 5403−5411.
Pace, C. N. (1992) *J. Mol. Biol. 226*, 29−35.
Pfeil, W. (1981) *Mol. Cell. Biochem. 40*, 3−28.
Pielak, G. J., Auld, D. S., Beasley, J. R., Betz, S. F., Cohen, D. S., Doyle, D. F., Finger, S. A., Fredericks, Z. L., Hilgen-Willis, S., Saunders, A. J., & Trojak, S. K. (1995) *Biochemistry 34*, 3268−3276.
Potekhin, S., & Pfeil, W. (1989) *Biophys. Chem. 34*, 55−62.
Privalov, P. L., & Khechinashvili, N. N. (1974) *J. Mol. Biol. 86*, 665−684.
Privalov, P. L., & Potekhin, S. A. (1986) *Methods Enzymol. 131*, 4−51.
Rafferty, S. P., Pearce, L. L., Barker, P. D., Guillemette, J. G., Kay, C. M., Smith, M., & Mauk, A. G. (1990) *Biochemistry 29*, 9365−9369.
Sachs, D. H., Schechter, A. N., Eastlake, A., & Anfinsen, C. B. (1972) *Proc. Natl. Acad. Sci. U.S.A. 69*, 3790−3794.
Sachs, D. H., Schecter, A. N., Eastlake, A., & Anfinsen, C. B. (1974) *Nature 251*, 242−244.
Sato, M., Yamamoto, M., Imada, K., Katsube, Y., Tanaka, N., & Higashi, T. (1992) *J. Appl. Crystallogr. 25*, 348−357.
Schellman, J. A. (1987) *Annu. Rev. Biophys. Biophys. Chem. 16*, 115−137.
Shirley, B. A., Stanssens, P., Hahn, U., & Pace, C. N. (1992) *Biochemistry 31*, 725−32.
Shortle, D., & Meeker, A. K. (1986) *Proteins 1*, 81−89.
Shortle, D., & Meeker, A. K. (1989) *Biochemistry 28*, 936−944.
Shortle, D., & Abeygunawardana, C. (1993) *Structure 1*, 121−134.
Sturtevant, J. M. (1987) *Annu. Rev. Phys. Chem. 38*, 463−488.
Tanaka, A., Flanagan, J., & Sturtevant, J. M. (1993) *Protein Sci. 2*, 567−576.
Taniguchi, V. T., Sailasuta-Scott, N., Anson, F. C., & Gray, H. B. (1980) *Pure Appl. Chem. 52*, 2275−2281.
Tong, H., Berghuis, A. M., Chen, J., Luo, Y., Guss, J. M., Freeman, H. C., & Brayer, G. D. (1994) *J. Appl. Crystallogr. 27*, 421−426.
Wilson, A. J. C. (1942) *Nature 150*, 151−152.
Wood, L. C., Muthukrishnan, K., White, T. B., Ramdas, L., & Nall, B. T. (1988) *Biochemistry 27*, 8554−8561.
Wynn, R., & Richards, F. M. (1993) *Biochemistry 32*, 12922−12927.
Zoller, M., & Smith, M. (1983) *Methods Enzymol. 100*, 1430−1437.
Zuniga, E. H., & Nall, B. T. (1983) *Biochemistry 22*, 1430−1437.
Zwanzig, R., Szabo, A., & Bagchi, B. (1992) *Proc. Natl. Acad. Sci. U.S.A. 89*, 20.

BI951228F